

## Supplementary Information

# A low crystallinity tungsten supported palladium catalyst and its electrochemical hydrogen evolution activity

*Yu Luo, Hanruo Chen, Wenjing Gao, Ying Li, Yingzhi Zhao, Hua Fang, Mingming Wang, Zhandong*

*Ren\* and Yuchan Zhu\**

Hubei Key Laboratory of Agricultural Waste Resource Utilization, School of Chemical and Environmental Engineering, Wuhan Polytechnic University, Wuhan, 430023, P. R. China.

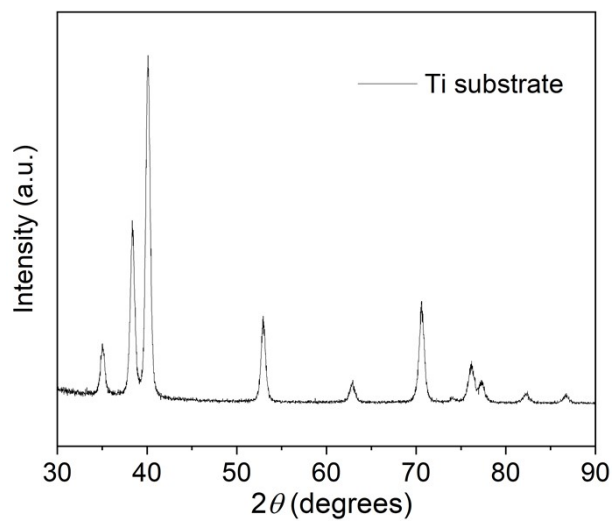


Figure S1 X-ray diffraction pattern of Ti substrate.

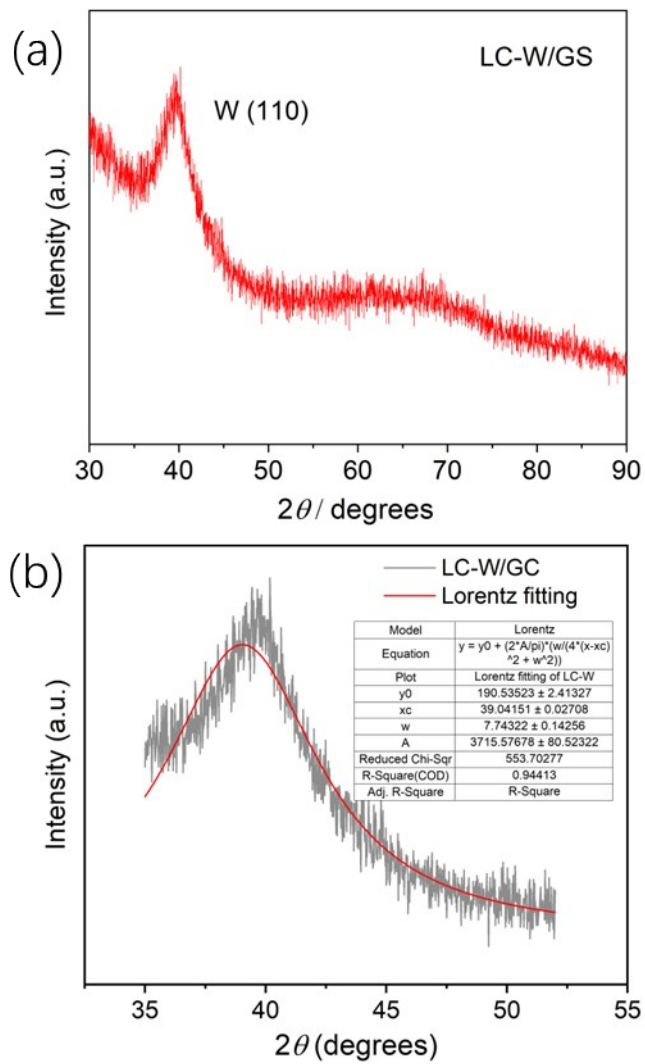


Figure S2 X-ray diffraction pattern (a) and fitting curve (b) of LC-W/GS.

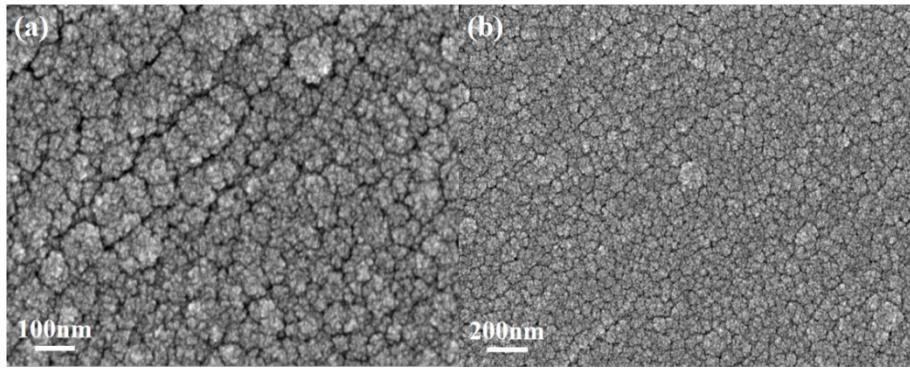


Figure S3 SEM images of LC-W/Ti.

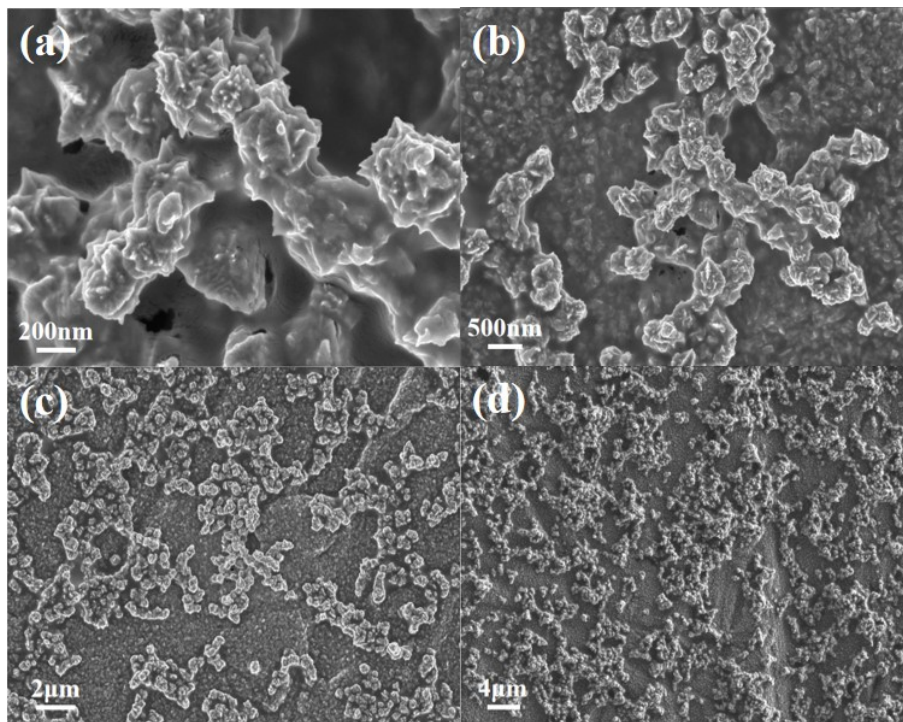


Figure S4 SEM images of Pd@LC-W/Ti.

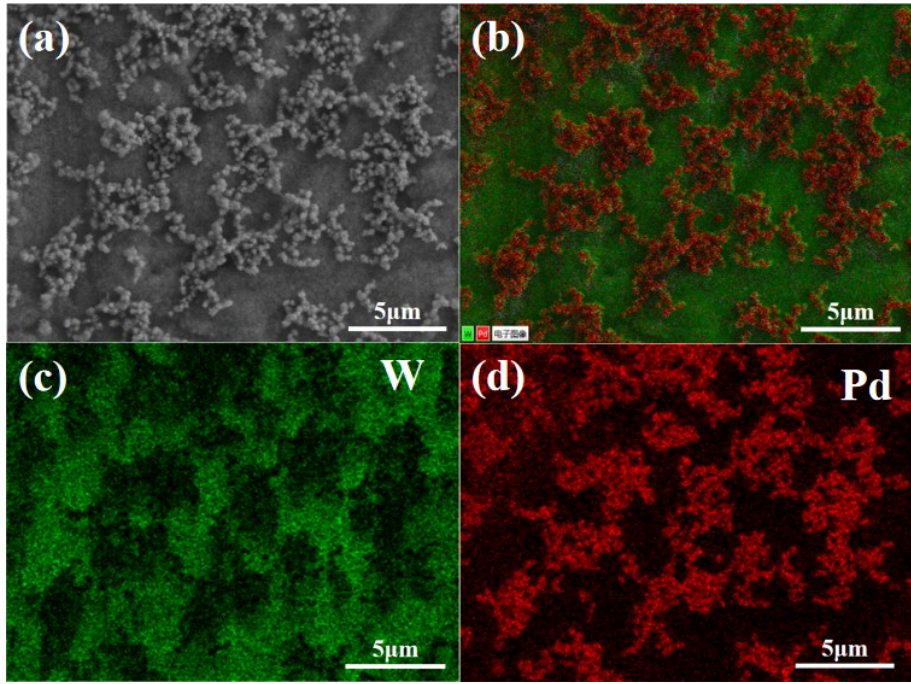


Figure S5 SEM-mapping of Pd@LC-W/Ti.

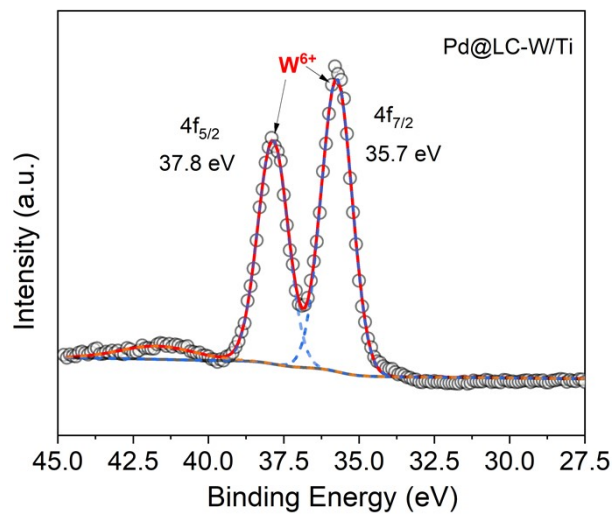


Figure S6 XPS core-level spectra of W 4f obtained from Pd@LC-W/Ti.

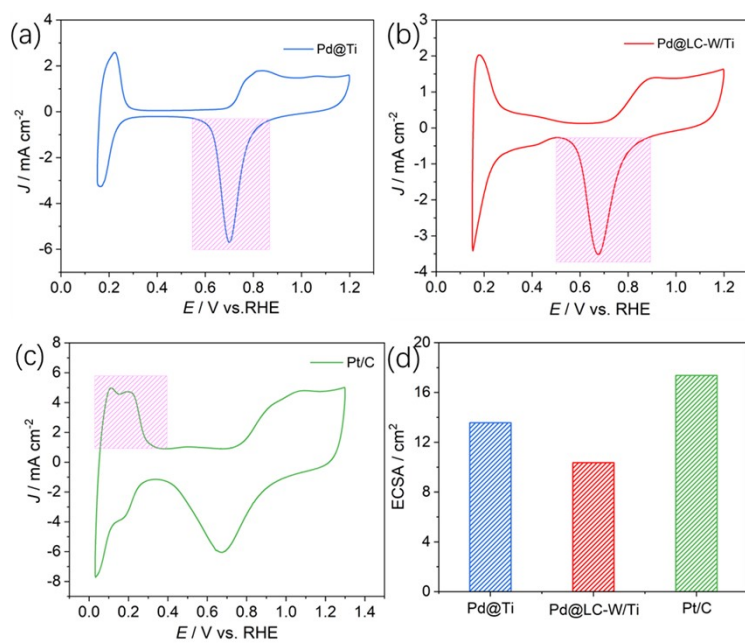


Figure S7 Electrochemical surface areas (ECSAs) of Pd@Ti, Pd@LC-W/Ti and Pt/C.

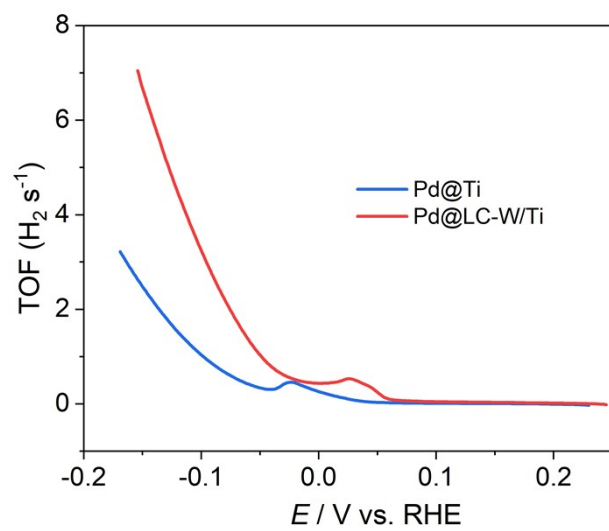


Figure S8 The turnover frequencies (TOFs) of Pd@Ti and Pd@LC-W/Ti.

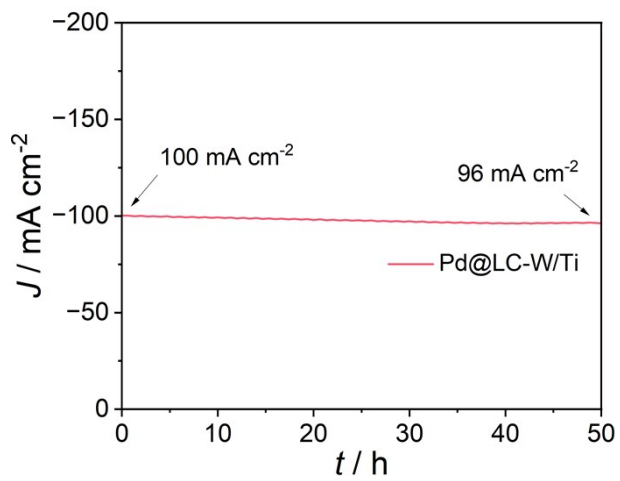


Figure S9 The stability of Pd@LC-W/Ti electrode.

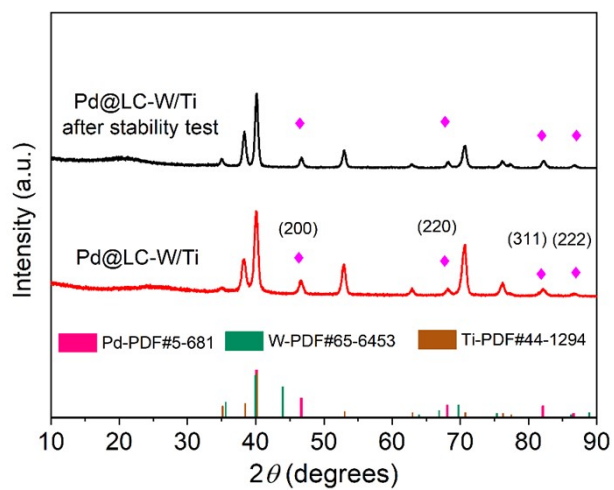


Fig. S10 X-ray diffraction patterns of Pd@LC-W/Ti before and after stability test.

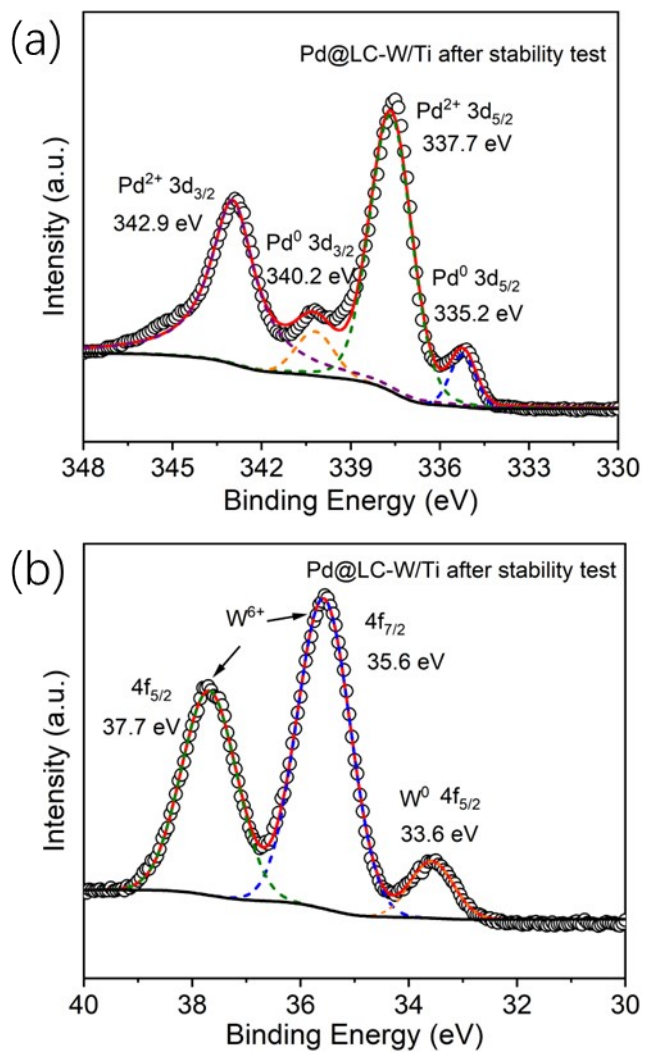


Fig. S11 XPS core-level spectra of Pd 3d (a) and W 4f (b) obtained from Pd@LC-W/Ti after stability test.

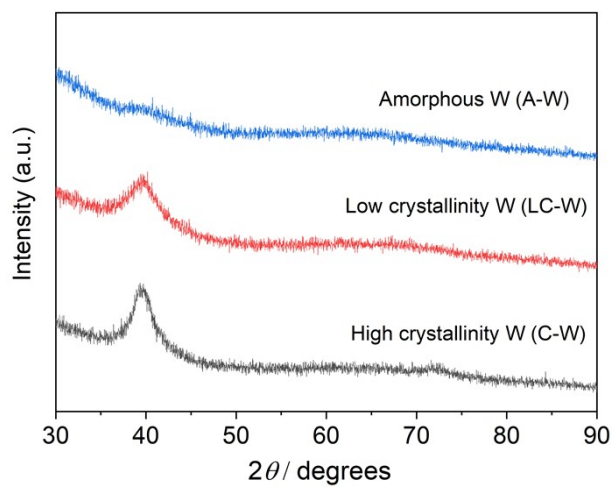


Figure S12 X-ray diffraction patterns of A-W, LC-W and C-W.

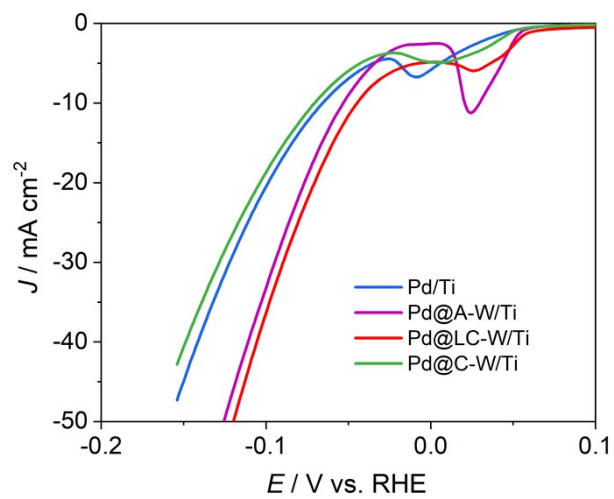


Figure S13 HER activities of Pd/Ti, Pd@A-W/Ti, Pd@LC-W/Ti and Pd@C-W/Ti.

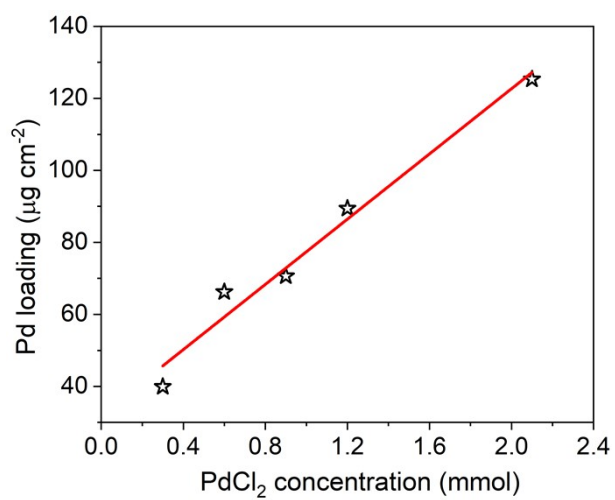


Figure S14 Relationship between PdCl<sub>2</sub> concentration and Pd loading.

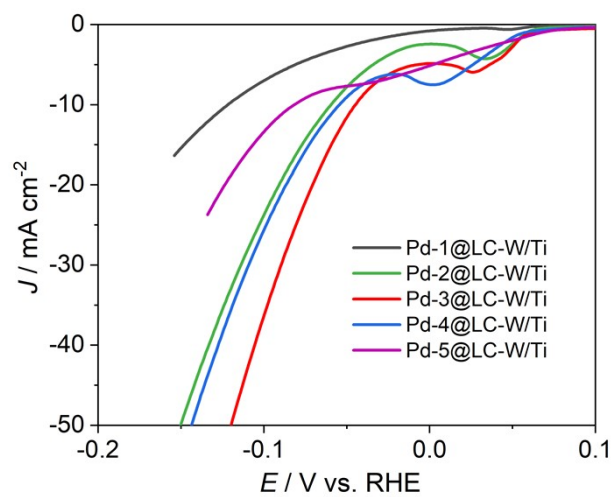


Figure S15 HER activities of Pd-x@LC-W/Ti with different Pd loadings.

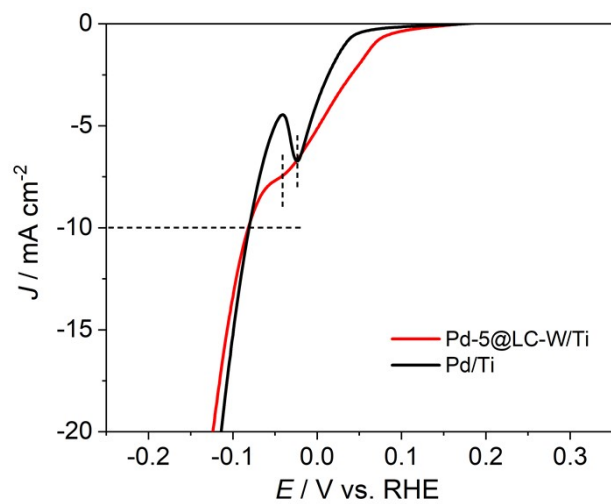


Figure S16 HER activities of Pd/Ti and Pd-5@LC-W/Ti.

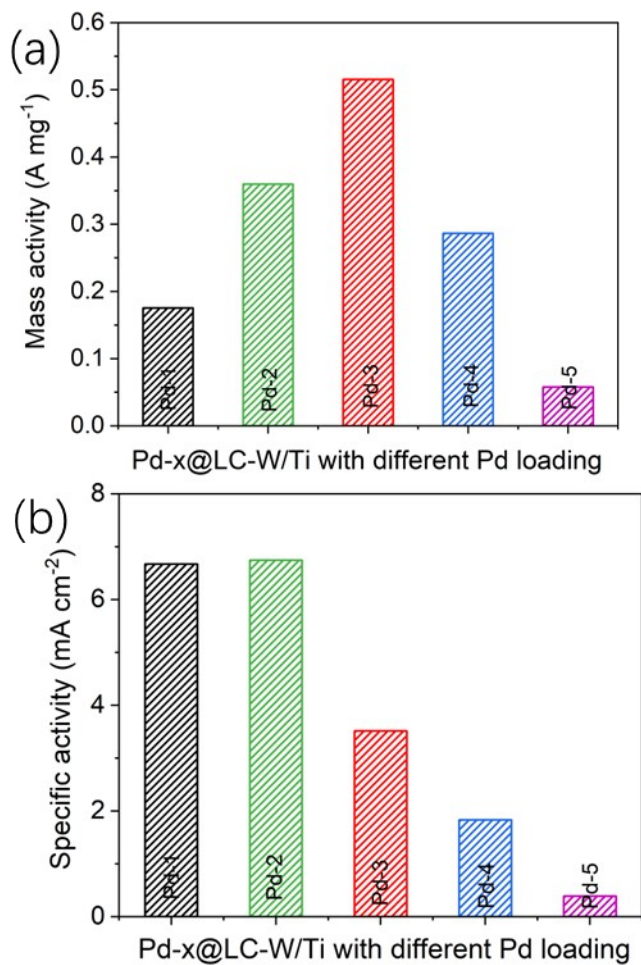


Figure S17 MA activities of Pd-x@LC-W/Ti with different Pd loadings.

Table S1 W Loading prepared at different sputtering times by XRF

Catalysts	Sputtering time (min)	W loading ( $\mu\text{g cm}^{-2}$ )
A-W/Ti	10	55.20
LC-W/Ti	20	126.1
C-W/Ti	40	259.8

Table S2 Pd loading of Pd-x@LC-W/Ti with different concentrations of PdCl<sub>2</sub>  
by XRF

Catalysts	concentrations of PdCl <sub>2</sub> (mol L <sup>-1</sup> )	Pd loading (μg cm <sup>-2</sup> )	W loading (μg cm <sup>-2</sup> )
Pd-1@LC-W/Ti	0.3 × 10 <sup>-3</sup>	39.90	
Pd-2@LC-W/Ti	0.6 × 10 <sup>-3</sup>	66.21	
Pd-3@LC-W/Ti	0.9 × 10 <sup>-3</sup>	70.60	259.8
Pd-4@LC-W/Ti	1.2 × 10 <sup>-3</sup>	89.37	
Pd-5@LC-W/Ti	2.1 × 10 <sup>-3</sup>	125.3	

Table S3 Overpotentials of Pd@Ti, Pd@LC-W/Ti and Pt/C at different current densities

Catalysts	$\eta_{10}$ (mV)	$\eta_{20}$ (mV)	$\eta_{40}$ (mV)
Pd@Ti	81	114	157
Pd@LC-W/Ti	45	71	106
Pt/C	33	48	76

Table S4 Comparison of HER activities between optimized Pd@LC-W/Ti and other Pd-based electrocatalysts in literatures. (0.5 M H<sub>2</sub>SO<sub>4</sub>)

Catalyst	$\eta_{10}$ (mV)	Tafel slope (mV dec <sup>-1</sup> )	Pd loading ( $\mu\text{g cm}^{-2}$ )	References
Cu@Pd	185	120	---	(1)
Pd-HPMo@GNP	94	90	15.5	(2)
Pd@MoS <sub>2</sub> /Mo <sub>2</sub> TiC <sub>2</sub> T <sub>x</sub>	92	60	---	(3)
Pd-PCNFs-800	93.1	88	71.4	(4)
NiCo <sub>2</sub> S <sub>4</sub> /Pd	87	70	43.0	(5)
Pd <sub>63</sub> Ni <sub>16</sub> Fe <sub>21</sub>	83	52	---	(6)
Pd <sub>83.5</sub> Ir <sub>16.5</sub>	73	43.6	75.2	(7)
PdKMX	72	69	8.8	(8)
Pd SA/WO <sub>3-x</sub>	70	68	13.8	(9)
Pd-MoS <sub>2</sub>	70	43	---	(10)
Ni-Pd/rGO	63	116	---	(11)
PdCo/SNC	58	75	70.0	(12)
PdI-RhI/MoS <sub>2</sub>	46	31	---	(13)
Pd, Re-MoS <sub>2</sub>	46	72	11.1	(14)
PdCuNi	45	33	---	(15)
PdRu <sub>x</sub> alloy	35.6	57	---	(16)
N-PdIr bimetallic	26	30.3	143	(17)
Pd <sub>3</sub> Sn/Ru	20	14	21.1	(18)
Pd@LC-W/Ti	45	82.9	70.6	This work

## References

1. V. Nithiyasri, K. Thulasi, P. S. Kumar. Hydrogen Evolution Reaction in Acidic, Neutral and Seawater Electrolyte Using Bimetallic Cu@Pd Core-Shell Nanostructures. *Adv. Sustainable Syst.*, **2026**, 10, e00738.

<https://doi.org/10.1002/adsu.202500738>

2. S. Iniyar, A. Vijayaprabakaran, C. Sebastian, M. Kathiresan. Modified Pd–HPMo@GNP as a highly effective electro-/nanocatalyst for the hydrogen evolution reaction and 4-nitrophenol reduction. *Materials Advances*, **2024**, 5, 7006–7015.

<https://doi.org/10.1039/d4ma00256c>

3. L. H. Zheng, C. K. Tang, Q. F. Lü, J. Wu. MoS<sub>2</sub>/Mo<sub>2</sub>TiC<sub>2</sub>T<sub>x</sub> supported Pd nanoparticles as an efficient electrocatalyst for hydrogen evolution reaction in both acidic and alkaline media. *Int. J. Hydrogen Energ.*, **2022**, 47, 11739–11749.

<https://doi.org/10.1016/j.ijhydene.2022.01.201>

4. Lu Li, Jiahao Gu, Yaqi Ye, Jun Guo, Jie Zhao, Guifu Zou. Effective synergy between palladium nanoparticles and nitrogen-doped porous carbon fiber for hydrogen evolution reaction. *Electrochim. Acta*, **2022**, 409, 139959.

<https://doi.org/10.1016/j.electacta.2022.139959>

5. G. Sheng, J. Chen, Y. Li, H. Ye, Z. Hu, X. Z. Fu, R. Sun, W. Huang, C. P. Wong. Flower-like NiCo<sub>2</sub>S<sub>4</sub> Hollow Sub-microspheres with Mesoporous Nanoshells Support Pd Nanoparticles for Enhanced Hydrogen Evolution Reaction Electrocatalysis in Both Acidic and Alkaline Conditions. *ACS Appl. Mater. Interfaces*, **2018**, 10, 22248–22256.

<https://doi.org/10.1021/acsami.8b05427>

6. P. Zou, L. Song, W. Xu, M. Gao, V. Zadorozhnyy, J. Huo, J. Q. Wang. High-throughput screening of superior hydrogen evolution reaction catalysts in Pd-Ni-Fe alloys. *J. Alloy. Compd.*, **2023**, 960, 170656.

<https://doi.org/10.1016/j.jallcom.2023.170656>

7. C. Wang, H. Xu, H. Shang, L. Jin, C. Chen, Y. Wang, M. Yuan, Y. Du. Ir-Doped Pd Nanosheet Assemblies as Bifunctional Electrocatalysts for Advanced Hydrogen Evolution Reaction and Liquid Fuel Electrocatalysis. *Inorg. Chem.*, **2020**, 59, 3321–3329.

<https://doi.org/10.1021/acs.inorgchem.0c00132>

8. Y. Sun, J. Lee, N. H. Kwon, J. Lim, X. Jin, Y. Gogotsi, S. J. Hwang. Enhancing Hydrogen Evolution Reaction Activity of Palladium Catalyst by Immobilization on MXene Nanosheets. *ACS Nano*, **2024**, 18, 6243–6255.

<https://doi.org/10.1021/acsnano.3c09640>

9. Z. Gong, Z. Chen, H. Li, G. Yang, M. Yuan, Z. Li, X. Wan, Y. Cui. Palladium single atoms from melting nanoparticles on  $\text{WO}_{3-x}$  for boosted hydrogen evolution reaction. *J. Energy Chem.*, **2024**, 91, 637–644.

<https://doi.org/10.1016/j.jechem.2023.11.033>

10. L. Mei, Y. Zhang, Z. Ye, T. Han, H. Hu, R. Yang, T. Ying, W. Zheng, R. Yan, Y. Zhang, Z. Wang, Z. Zeng. Fabrication of Amorphous Subnanometric Palladium Nanostructures on Metallic Transition Metal Dichalcogenides for Efficient Hydrogen Evolution Reaction. *Inorg. Chem. Front.*, **2024**, 11, 3838–3847.

<https://doi.org/10.1039/D4QI00622D>

11. A. Prytkova, M. A. Kirsanova, A. G. Kiiamov, D. A. Tayurskii, A. M. Dimiev. Ni–Pd Nanocomposites on Reduced Graphene Oxide Support as Electrocatalysts for Hydrogen Evolution Reactions. *ACS Appl. Nano Mater.*, **2023**, 6, 14902–14909.

<https://doi.org/10.1021/acsanm.3c02461>

12. C. Renugadevi, L. Cindrella. Nanoscale Pd-Co alloy supported on dual heteroatoms doped carbon-An efficient electrocatalyst for hydrogen evolution and oxygen reduction reactions. *J. Alloy. Compd.*, **2025**, 1022, 179990.

<https://doi.org/10.1016/j.jallcom.2025.179990>

13. M. Sookhakian, R. Siburian, G. B. Tong, M. A. M. Teridi, E. Mahmoud, Y. Alias. Ratio design of bimetallic Pd-Rh nanoparticles on  $\text{MoS}_2$  nanosheets: Excellent electrocatalysts for hydrogen evolution reaction. *Appl Organomet Chem.*, **2024**, 38, e7541.

<https://doi.org/10.1002/aoc.7541>

14. Z. Luo, J. Li, Y. Li, D. Wu, L. Zhang, X. Ren, C. He, Q. Zhang, M. Gu, X. Sun. Band Engineering Induced Conducting 2H-Phase  $\text{MoS}_2$  by Pd-S-Re Sites Modification for Hydrogen Evolution Reaction. *Adv. Energy Mater.*, **2022**, 12, 2103823.

<https://doi.org/10.1002/aenm.202103823>

15. X. Liu, H. Pang, X. Kou, Z. Tang, B. Cui, S. Cen, Y. Wei. Synergistic interaction of ternary Pd–Cu–Ni confined in nanoparticles as pH-universal catalysts for enhanced hydrogen evolution reaction. *Chinese Chem. Lett.*, 2026, 37, 111567.

<https://doi.org/10.1016/j.cclet.2025.111567>

16. Y. Liu, T.-Q. Zi, Y. Huang, S. Zhang, J. A. S. Syed, L. Gao, W.-M. Li, A.-D. Li. Atomic Layer Deposition of PdRu<sub>x</sub> Alloy Nanoparticles for Hydrogen Evolution Reaction Electrocatalysis in Acidic Media. *ACS Appl. Nano Mater.*, 2025, 8, 8807–8815.

<https://doi.org/10.1021/acsnm.5c00794>

17. Q. Mao, K. Deng, W. Wang, P. Wang, Y. Xu, Z. Wang, X. Li, L. Wang, H. Wang. N-doping induced lattice-strained porous PdIr bimetallic for pH-universal hydrogen evolution electrocatalysis. *J. Mater. Chem. A*, 2022, 10, 8364–8370.

<https://doi.org/10.1039/d2ta00590e>

18. M. Su, S. Qiu, Y. Zhang, Y. Zhao, X. Chen, Y. Ding, I. Rehman, K. Tao, E. Xie, Z. Zhang. Interface charge engineering in Pd<sub>3</sub>Sn/Ru heterostructures for ultra-efficient wide-pH hydrogen evolution. *J. Colloid Interface Sci.*, **2026**, 703, 139166.

<https://doi.org/10.1016/j.jcis.2025.139166>

Table S5 Comparison of HER activities between optimized Pd@LC-W/Ti and other Ti-based electrocatalysts in literatures.

Catalyst	Electrolyte	$\eta_{10}$ (mV)	Tafel slope (mV dec <sup>-1</sup> )	Reference s
Pd-WO <sub>3</sub> /W/Ti	0.5 M H <sub>2</sub> SO <sub>4</sub>	52	80.6	(1)
(Pt <sub>a</sub> c-O-Au)-1/Ti	0.5 M H <sub>2</sub> SO <sub>4</sub>	41	28.6	(2)
N-MXene-35/Ti	0.5 M H <sub>2</sub> SO <sub>4</sub>	162	69	(3)
MoS <sub>2</sub> /MnMoO <sub>4</sub> @Ti	0.5 M H <sub>2</sub> SO <sub>4</sub>	153	80	(4)
GNWs/Mo-MXene/Ti	0.5 M H <sub>2</sub> SO <sub>4</sub>	132	178	(5)
TiH <sub>2</sub> /Ti	0.5 M H <sub>2</sub> SO <sub>4</sub>	224	202.4	(6)
Pt@Ti <sub>3</sub> C <sub>2</sub> T <sub>x</sub>	0.5 M H <sub>2</sub> SO <sub>4</sub>	60.8	59.2	(7)
core-shell VS <sub>2</sub> /Ti <sub>3</sub> C <sub>2</sub>	0.5 M H <sub>2</sub> SO <sub>4</sub>	59	38.42	(8)
Ru/Ni-NiO/Mo <sub>2</sub> TiC <sub>2</sub> T <sub>x</sub>	0.5 M H <sub>2</sub> SO <sub>4</sub>	49	62	(9)
CoP/Ti <sub>3</sub> C <sub>2</sub> T <sub>x</sub>	0.5 M H <sub>2</sub> SO <sub>4</sub>	135	48	(10)
Pd@LC-W/Ti	0.5 M H <sub>2</sub> SO <sub>4</sub>	45	82.9	This work

1. Y. Xin, H. Chen, H. Ye, Z. Xie, Q. Ma, S. Yu, Y. Zhu, Z. Ren. Influence of hydrogen spillover effect on hydrogen absorption/desorption and electrochemical hydrogen evolution activity of Pd-WO<sub>3</sub>/W. *J. Electroanal. Chem.*, 2026, 1000, 119623.

2. Z. Ren, Z. Xie, L. Deng, C. Dong, G. Song, X. Liu, J. Han, L. Zhuang, Y. Liu, Y. Zhu. Ultra-low loading Pt atomic cluster electrode with Pt-O bond as an active site with high hydrogen evolution reaction performance. *Inorg. Chem. Front.*, 2023, 10, 1101–1111.

3. M. Han, J. Yang, J. Jiang, 2R. Jing, S. Ren, C. Yan. Efficient tuning the electronic structure of N-doped Ti-based MXene to enhance hydrogen evolution reaction. *J. Colloid Interface Sci.*, 2021, 582, 1099–1106.

<https://doi.org/10.1016/j.jcis.2020.09.001>

4. J. G. Badiger, M. Arunachalam, R. S. Kanase, S. A. Sayed, K.-S. Ahn, J.-S. Ha, S. H. Kang. Highly stable MoS<sub>2</sub>/MnMoO<sub>4</sub>@Ti nanocomposite electrocatalysts for hydrogen evolution reaction.

- Int. J. Hydrogen Energy*, 2024, 51, 156–168.  
<https://doi.org/10.1016/j.ijhydene.2023.08.091>
5. J. Serafin, G. Farid, S. Chaitoglou, S. Majumdar, A. Pérez del Pino, E. Gyorgy, R. Amade-Rovira, Y. Ma, X. Vendrell, A. Sánchez, E. Bertran-Serra, N. Homs. Hierarchical graphene nanowalls/Ti, Mo–MXene nanocomposites for enhanced electrocatalytic hydrogen evolution. *Int. J. Hydrogen Energy*, 2025, 165, 150886.  
<https://doi.org/10.1016/j.ijhydene.2025.150886>
6. D. Jiang, L. Yang, H. Yuan, L. Zhao, J. Yu, X. Liu, Y. Wang, T. Zhang, T. Dong, M. Huang, Z. Liu, W. Zhou, H. Liu. Saturated hydrogen regulated ti coordination of metallic TiH<sub>2</sub>/Ti electrode via in-situ electrochemical hydrogenation for enhanced hydrogen evolution reaction. *Nano Energy*, 2022, 93, 106892.  
<https://doi.org/10.1016/j.nanoen.2021.106892>
7. D. Yang, Y. Wang, X. Liu, Y. Gao, Y. Chen, G. Tian, S. Wang, L. Zhang, N. Tang. Titanium-vacancy-based Ti<sub>3</sub>C<sub>2</sub>T<sub>x</sub> MXene with In-Situ Loaded ultra-low platinum demonstrating outstanding hydrogen evolution performance in acidic seawater. *Electrochim. Acta*, 2025, 536, 146759.  
<https://doi.org/10.1016/j.electacta.2025.146759>
8. K. Zhao, Y. Zhang, S. Liu, Q. Gao, Y. Zhang, S. Wei, T. Zhou, Y. Feng, Q. Lu. A core-shell VS<sub>2</sub>/Ti<sub>3</sub>C<sub>2</sub> heterojunction electrocatalyst for efficient hydrogen evolution. *Int. J. Hydrogen Energy*, 2026, 206, 153396.  
<https://doi.org/10.1016/j.ijhydene.2026.153396>
9. S. Liu, L. Liu, J. Liu, Y. Xiang, L. Gao, F. Fu, X. Gao, X. Jian. Mo<sub>2</sub>TiC<sub>2</sub>T<sub>x</sub> MXene-Supported RuNi–NiO as an Electrocatalyst for the pH-Universal Hydrogen Evolution Reaction. *ACS Appl. Nano Mater.*, 2023, 6, 20446–20456.  
<https://doi.org/10.1021/acsanm.3c04420>
10. W. Sun, Y. Wang, K. Xiang, S. Bai, H. Wang, J. Zou, Arramel, J. Jiang. CoP Decorated on Ti<sub>3</sub>C<sub>2</sub>T<sub>x</sub> MXene Nanocomposites as Robust Electrocatalyst for Hydrogen Evolution Reaction. *Acta Phys. -Chim. Sin.*, 2024, 40, 2308015.  
<https://doi.org/10.3866/PKU.WHXB202308015>

Table S6 Fitting parameters in the equivalent circuit of Pd@Ti and Pd@LC-W/Ti

Catalysts	$R_s / \Omega \text{ cm}^2$	$R_{ct} / \Omega \text{ cm}^2$	$C_{dl} / \text{mC cm}^{-2}$
Pd@Ti	0.306	16.430	0.576
Pd@LC-W/Ti	0.300	4.388	0.412

Table S7 Pd loading of Pd@LC-W/Ti before and after stability test

Catalysts	Stability test	Pd loading ( $\mu\text{g cm}^{-2}$ )
Pd@LC-W/Ti	/	70.60
Pd@LC-W/Ti	100 mA $\text{cm}^{-2}$ 50 h test	65.17

